ORIGINAL ARTICLE

Supplemental information
Quantum Nuclei at Weakly Bonded Interfaces: The Case of Cyclohexane on Rh(111)

Karen Fidanyan[1,2] | **Ikutaro Hamada**[3] | **Mariana Rossi**[1,2]

[1]Fritz-Haber-Institut der Max-Planck-Gesellschaft, Faradayweg 4-6, 14195 Berlin, Germany

[2]Max Planck Institute for Structure and Dynamics of Matter, Luruper Chaussee 149, 22761 Hamburg, Germany

[3]Department of Precision Engineering, Graduate School of Engineering, Osaka University, 2-1 Yamadaoka, Suita, Osaka 565-0871, Japan

Correspondence
Email:

Funding information

Supplemental information

1 | ADSORPTION PROPERTIES

Adsorption energies $E_{\text{ads}}^{\text{pot}}$ for the systems discussed in the paper are provided in table S1.

A comparison of the adsorption energy curve between *Light* and *Tight* settings is provided in figure S1 for $\theta = 0.46$. The difference in binding energy is 58 meV.

As mentioned in the paper, we use E_{ads} calculated by the eq. 5 and E_{ads}^{*} calculated by the eq. 7. Only E_{ads} rigorously satisfies the definition of an adsorption energy. Comparing the numbers for coverage 0.46 and PBE + vdW$^{\text{surf}}$ in tables S1 and S2, one can compare the values obtained with these two definitions. The differences are very small (less than 10 meV).

TABLE S1 Adsorption energy for different adsorption patterns, calculated with PBE+vdW^{surf} by FHI-aims code with *Light* and *Tight* settings.

	$E_{ads}\left(\frac{eV}{molecule}\right)$
θ = 1, $\left(2\sqrt{3}\times 2\sqrt{3}\right)R13.9^{\circ}$, 9 molecules, 4 Rh layers	
Light, 2x2x1 k-points	1.023
θ = 0.64, 3x3 slab with 1 molecule	
Light, 4x4x1 k-points	0.946
θ = 0.46, 5x5 slab with 2 molecules	
Light, 2x2x1 k-points	0.953
Tight, 2x2x1 k-points	0.912
θ = 0.12, 7x7 slab with 1 molecule	
Light, 2x2x1 k-points	0.945

TABLE S2 Adsorption distance h_{COM} between the center of mass of a molecule and a surface, and energy E^{*}_{ads}, calculated as the energy difference between the minimal point of the adsorption curve and the point at 10 Å distance from the surface.

FHI-aims	h_{COM} (Å)	E^{*}_{ads} (meV)
θ = 0.46**, *Tight* settings**		
PBE	3.71	147
PBE+MBD-nl	3.45	843
PBE + vdW^{surf}	3.36	905
HSE06+MBD-nl	3.30	1026
θ = 0.46**, *Light* settings**		
PBE + vdW^{surf}	3.37	963

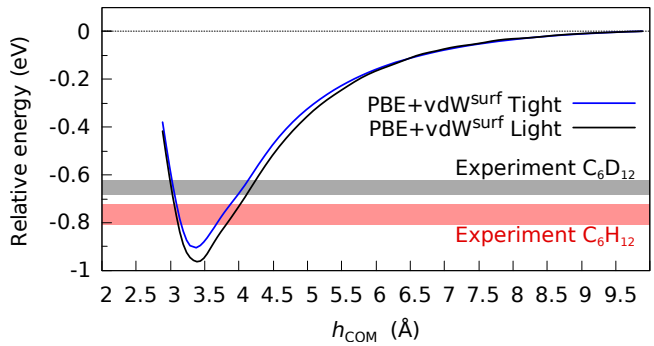

FIGURE S1 Adsorption curves calculated with PBE +vdW^{surf} [1] functional with *Tight* (solid blue line) and *Light* (dashed black line) settings of FHI-aims. Calculations were performed with the unit cell of $\theta = 0.46$. Shaded areas show the experimental values of the adsorption energy of C_6H_{12} (red) and C_6D_{12} (grey), obtained by temperature programmed desorption [2].

2 | COVERAGE DEPENDENCE OF VIBRATIONAL SPECTRUM

We show in figure S2 the harmonic vDOS for the adsorption patterns considered in this work (PBE+vdW^{surf}). The key feature is a red shift in the stretching vibrations of the CH groups pointing to the surface (denoted as (I) in figure S2b). This red shift decreases with increasing coverage. It means that surface-molecule interaction becomes weaker. At highest coverage (θ = 1) there are multiple splittings of CH stretching frequencies. It is an evidence that cyclohexane adsorption sites become highly nonequivalent because of molecule-molecule interactions. We also note a blue shift in stretching vibrations of CH groups of type (III) and slight red shift in groups (II) and (IV).

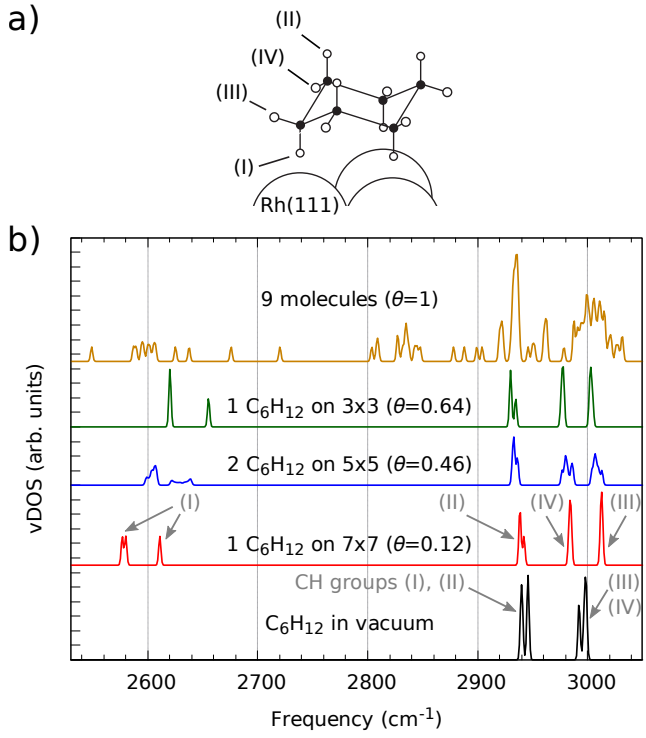

FIGURE S2 a) Different CH groups for a cyclohexane adsorbed on a surface. b) The vibrational spectra of CH stretching modes of cyclohexane in vacuum (black) and on a Rh(111) surface with coverage θ = 0.12 (red), θ = 0.46 (blue), θ = 0.64 (green) and θ = 1 (ochre). The grey arrows assign peaks to the CH groups given in (b). As the red shift in CH stretching modes decreases, the H/D difference in the adsorption energy decreases also. At the full coverage (θ = 1), the intermolecular interaction is so strong that single adsorption sites become highly non-equivalent, which is reflected in multiple peak splitting in the range between 2540 and 3040 cm^{-1}.

3 | CALCULATIONS WITH REV-VDW-DF2 FUNCTIONAL

The Quantum-ESPRESSO code [3, 4] was used for the calculations of adsorption energy curve without zero-point-energy correction as a function of molecule-surface distance with a Rh(111) (3×3) surface with 4 metal layers and vacuum equivalent to eight monolayer (19.77 Å) with rev-vdW-DF2 functional as shown in figure S3 (a) ($\theta = 0.64$). A 6×6 Γ-centered k-point grid was used. The results for $\theta = 0.46$ and $\theta = 0.64$ are given in table S3.

The STATE [5, 6] code was used for the calculations of vibrational spectra, adsorption energy curves with and without zero-point-energy correction, and the work function as functions of the molecule-surface distance with the rev-vdW-DF2 functional[7, 8]. A simplified version of the self-consistent van der Waals density functional[9, 10] was employed[11]. The computational setup for the STATE calculations has multiple differences from the one reported in the main text. For these calculations, a Rh(111) (3×3) surface with 5 metal layers with a vacuum equivalent to eight monolayer (19.88 Å) is considered ($\theta = 0.64$). The slab was constructed using the lattice constant optimized with rev-vdW-DF2 of 3.81 Å. A cyclohexane molecule was put on one side of the slab and the effective screening medium method was used to eliminate the artificial electrostatic interaction with the neighboring slabs [12, 13]. The bottom 2 layers of the Rh(111) slab were fixed and the remaining degrees of freedom were fully relaxed until the forces acting on them become less than 5×10^{-4} Hartree/Bohr. Ultrasoft pseudopotentials [14] and a plane-wave basis sets with a cutoff energy of 49 (625) Ry for wave functions (charge density) were used. A 4×4 Γ-centered k-point grid was used. Harmonic vibrational frequencies were calculated by using the Wilson's GF method and finite difference method as implemented in the STATE package[15]. Atoms were displaced along the vibrational eigenmodes and the magnitude of the displacement was determined self-consistently. All $3N$ molecular vibrations are included in zero-point energy calculation. The results are presented in figure S3 (b) and in table S4.

TABLE S3 Adsorption distance h_{COM} between the center of mass of a molecule and a surface, and energy E_{ads}, calculated as the energy difference between the minimal point of the adsorption curve and the sum of energies of an isolated molecule and a clean surface using Quantum ESPRESSO.

Quantum ESPRESSO	h_{COM} (Å)	E_{ads} (meV)
$\theta = 0.46$, rev-vdW-DF2	3.48	768
$\theta = 0.64$, rev-vdW-DF2	3.49	791

TABLE S4 The results of quasi-harmonic calculation with rev-vdW-DF2: the adsorption energy, the equilibrium distance between molecules and the surface, and the work function change for C_6H_{12} and C_6D_{12} for coverage $\theta = 0.64$ using STATE.

STATE	C_6H_{12}	C_6D_{12}	no ZPE
ZPE-corrected E_{ads} (meV)	876	840	818
QH h_{COM} (Å)	3.427	3.439	3.471
QH $\Delta\phi$ (meV)	-1205	-1190	-1151

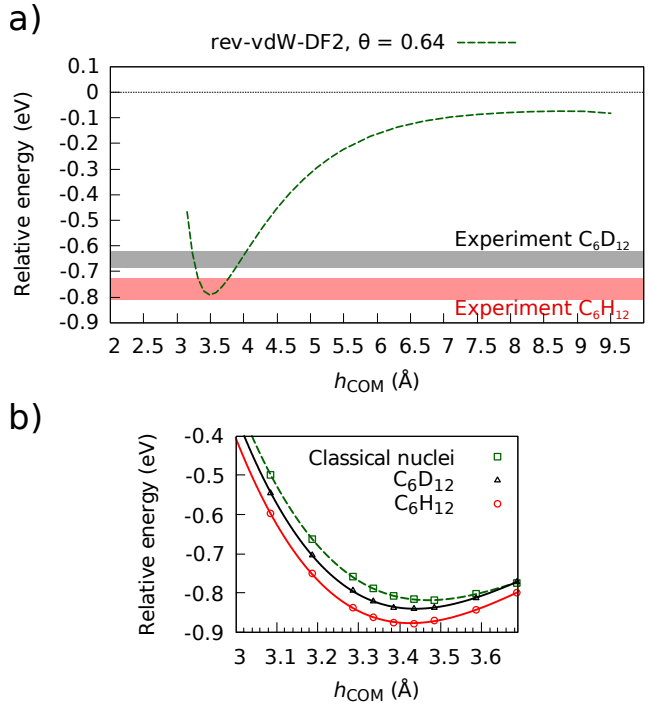

FIGURE S3 a) Adsorption curve calculated with rev-vdW-DF2 for the coverage of $\theta = 0.64$ obtained using Quantum-ESPRESSO. Zero energy level corresponds to sum of the energies of an isolated molecule and a clean surface. Shaded areas show the experimental values of the adsorption energy of C_6H_{12} (red) and C_6D_{12} (grey), obtained by temperature programmed desorption [2]. b) ZPE-corrected energy of adsorption for C_6H_{12} (red) and C_6D_{12} (black) obtained with STATE. The green line shows the adsorption energy values calculated without ZPE correction. Zero level is the same as in a).

TABLE S5 Isotope effects on distance to surface and work function change, obtained by QH model and aiPIMD simulations with PBE + vdW^{surf} functional for coverage $\theta = 0.46$.

	C_6H_{12}	C_6D_{12}	no ZPE
ZPE-corrected E^*_{ads} (meV)	1067	1030	956
QH h_{COM} (Å)	3.351	3.364	3.386
QH $\Delta\phi$ (meV)	-960	-945	-920
PIMD h_{COM} (Å)	3.41 ± 0.01	3.42 ± 0.01	3.416 ± 0.007
PIMD $\Delta\phi$ (meV)	-927 ± 9	-915 ± 9	-903 ± 5

4 | QUASI-HARMONIC MODEL AT FINITE TEMPERATURE

For the calculation of a ZPE corrected adsorption curves, with FHI-aims we include only $(3N_m - 3)$ molecular vibrations, where N_m is the number of atoms in a molecule. The remaining 3 lowest-frequency modes (0 to 55 cm^{-1} depending on distance to surface) correspond to the hindered translations of a rigid molecule. They have completely classical behavior and high entropy, and they are populated at very low temperatures. These modes give a relatively high mobility to molecules. They raise the question of applicability of the harmonic approximation when the molecule deviates far away from its equilibrium position.

In figures S4a,b, we show harmonic free energy corrections at 150 K including $(3N_m - 3)$ modes and only the $(3N_m - 6)$ intramolecular modes. Clearly, temperature effects are concentrated in the lower-frequency modes, and these effects are negligibly small in the higher frequency intramolecular vibrations. h_{COM} when including $(3N_m - 3)$ modes is **3.351 (3.365)** Å for H and **3.364 (3.384)** Å for D at the temperature of 0 (150) K.

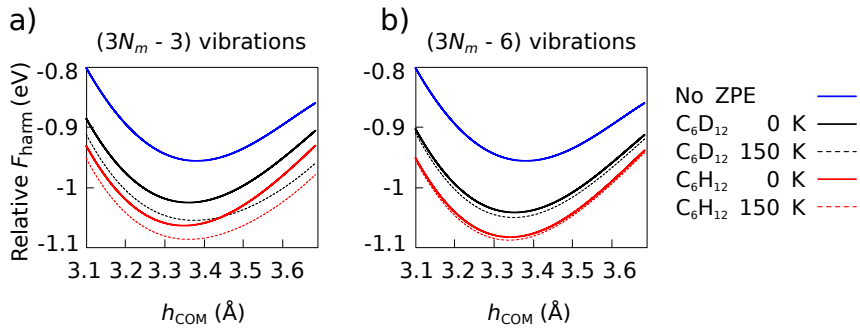

FIGURE S4 The effect of temperature on the harmonic free energy of cyclohexane (red) and D-cyclohexane (black) with and without inclusion of hindered rigid rotation modes (a and b, respectively). Solid lines show ZPE-corrected potential energy, dashed lines add finite temperature corrections at the temperature of 150 K. The curves are aligned to zero at the distance of 10 Å. Calculations are done with PBE + vdW^{surf} functional.

5 | DEPENDENCE OF THE WORK FUNCTION CHANGE ON COVERAGE AND FUNCTIONAL

We have calculated the dependence of work function change on distance for the coverage 0.64 using rev-vdW-DF2 and PBE functionals. The results are shown in figure S5. Taking the slope of the rev-vdW-DF2 dependence, the QH model predicts the isotopic difference in work function change to be **15 meV** (see table S4). In addition, we show the difference between self-consistent and non-self-consistent implementations of vdW^{surf} correction in the work function [16].

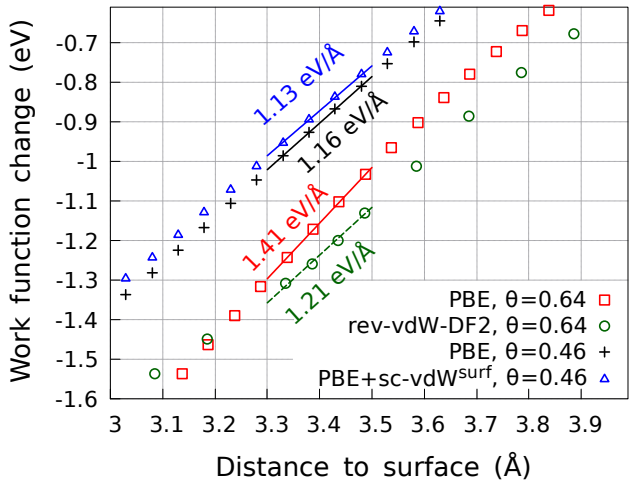

FIGURE S5 Work function change as a function of distance to surface. Calculated for coverage 0.64 using PBE (red squares) and rev-vdW-DF2 (green circles) functionals. And the values for coverage 0.46 by PBE (black crosses) and PBE + self-consistent vdW^{surf} (blue triangles).

6 | ELECTRON DENSITY REARRANGEMENT

Multiple slices of the electron density difference between the full system (surface+molecules) and the superposition of an isolated adsorbate and a clean surface are presented (figures S6, S7). In these pictures, shades of blue mean electron depletion upon adsorption, and shades of red mean electron accumulation.

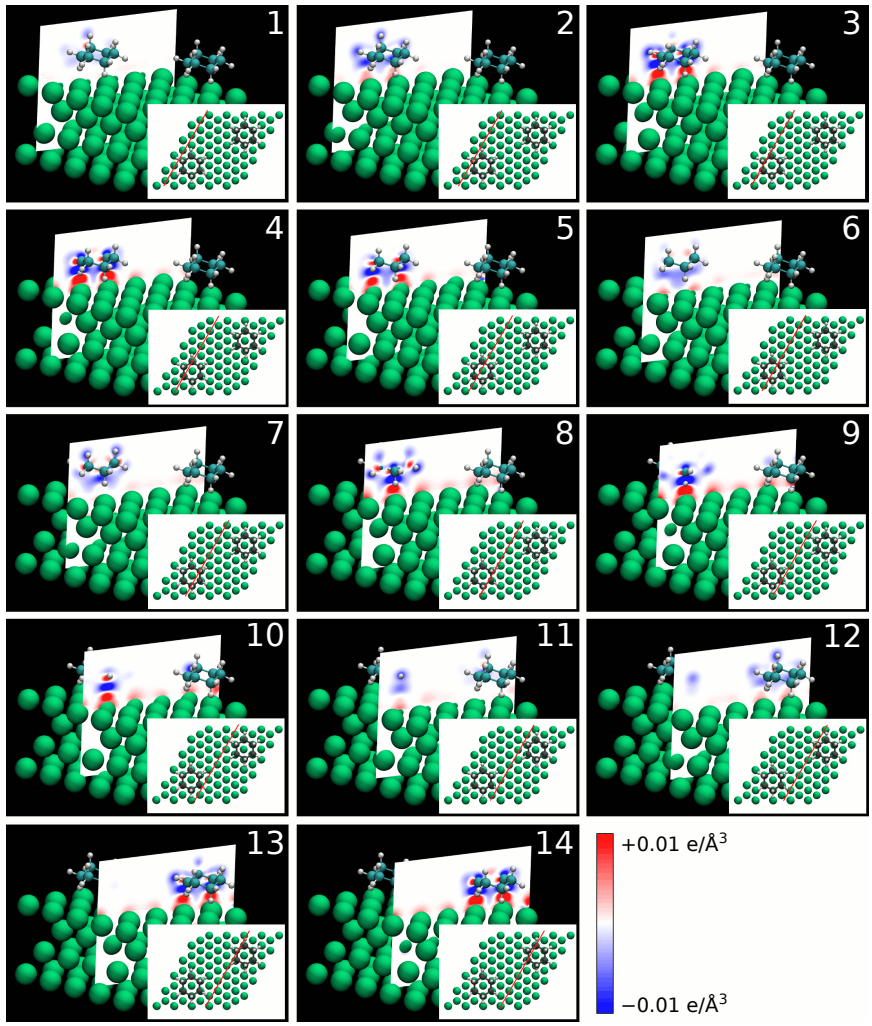

FIGURE S6 Difference between the electron density of a surface with molecules adsorbed and the sum of isolated surface and isolated molecules, shown at different $y - z$ slices along x coordinate. Red color denotes electron density accumulation, and blue denotes depletion.

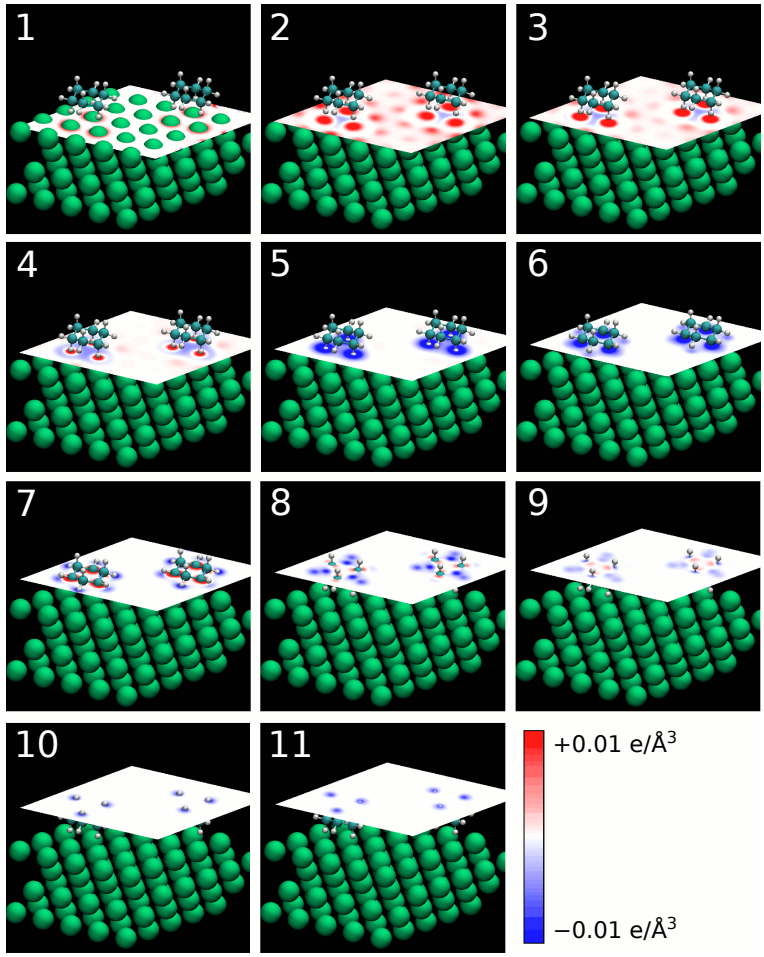

FIGURE S7 Difference between the electron density of a surface with molecules adsorbed and the sum of isolated surface and isolated molecules, shown at different $x - y$ slices along z coordinate. Red color denotes electron density accumulation, and blue denotes depletion.

7 | ESTIMATE OF THE ERROR OF SL-RPC IN POTENTIAL ENERGY

Our expression 2 in the manuscript can be rewritten as

$$\frac{k_B T}{2} \sum_{\nu} \sum_{k} \left[\frac{\omega_{\text{mol}}^2}{\omega_k^2 + \omega_{\nu,\text{full}}^2 + \Delta} - \frac{\omega_{\text{full}}^2}{\omega_k^2 + \omega_{\nu,\text{full}}^2} \right], \tag{1}$$

where $\Delta = \omega_{\nu,\text{mol}}^2 - \omega_{\nu,\text{full}}^2$. Since Δ is much smaller than $\omega_k^2 + \omega_{\nu,\text{full}}^2$, it can be omitted, and we immediately get eq. 9 from the Ref. [17]. It is a reasonable approximation of one fraction, which gives an error of not more than 10% in practical cases. However, two fractions have quite close values, therefore the *difference* between them can be even smaller than the error introduced by omitting the Δ. This fact leads to a significant overestimation of the error, if the eq. 9 from [17] is used.

8 | ESTIMATE OF THE ERROR OF SL-RPC IN FREE ENERGY

Assuming a system to be harmonic, the Hamiltonian of a ring polymer with P beads in "physical" normal modes can be written as

$$H = K + \sum_{\nu=1}^{3N} \sum_{k=1}^{P} \left[\frac{m_\nu \omega_P^2}{2} \left(q_\nu^{(k)} - q_\nu^{(k+1)} \right)^2 + \frac{m_\nu \omega_\nu^2}{2} q_\nu^{(k)2} \right]. \tag{2}$$

Here K is a kinetic energy, ν denotes normal modes (NMs) of a physical system, m_ν is an effective mass associated with the normal mode ν. Note that here, k stands for a bead index – in contrast to the following equations, where it will enumerate normal modes of a free ring polymer.

Expanding the spring-terms and rearranging the summation over k (also making use of periodicity of a ring polymer $q^{(P+1)} = q^{(1)}$), one can rewrite a Hamiltonian as following:

$$H = K + \sum_{\nu=1}^{3N} \sum_{k=1}^{P} \left[\frac{m_\nu \omega_P^2}{2} \left(2q_\nu^{(k)2} - q_\nu^{(k)} q_\nu^{(k+1)} - q_\nu^{(k)} q_\nu^{(k-1)} \right) + \frac{m_\nu \omega_\nu^2}{2} q_\nu^{(k)2} \right]. \tag{3}$$

Then, the spring terms can be written in a matrix form (bold below means P-dimensional vectors $\{q^j\}, j \in [1, ..., P]$ and corresponding square matrices)

$$V^{spring} = \sum_{\nu=1}^{3N} \frac{m_\nu \omega_P^2}{2} \boldsymbol{q}_\nu^\top \boldsymbol{A} \boldsymbol{q}_\nu, \tag{4}$$

$$\boldsymbol{A} = \begin{bmatrix} 2 & -1 & 0 & \dots & & -1 \\ -1 & 2 & -1 & 0 & & \\ 0 & -1 & 2 & \dots & & \\ \dots & 0 & \dots & & & \\ & & & & & -1 \\ -1 & & & & -1 & 2 \end{bmatrix} \tag{5}$$

We diagonalize the $\boldsymbol{A}$ matrix by performing a normal mode transformation $\boldsymbol{C}$:

$$\boldsymbol{A} = \boldsymbol{C}\tilde{\boldsymbol{A}}\boldsymbol{C}^{\top}. \tag{6}$$

$$\tilde{\boldsymbol{q}}_v = \boldsymbol{C}\boldsymbol{q}_v \tag{7}$$

The matrix $\boldsymbol{C}$ is unitary, therefore the transformation to the normal modes of a free ring polymer doesn't change the physical potential term

$$\frac{m_v\omega_v^2}{2}\boldsymbol{q}_v^2 = \frac{m_v\omega_v^2}{2}\tilde{\boldsymbol{q}}_v^{\top}C^{-1\top}C^{-1}\tilde{\boldsymbol{q}}_v = \frac{m_v\omega_v^2}{2}\tilde{\boldsymbol{q}}_v^2. \tag{8}$$

The Hamiltonian in the "double normal-mode" representation (i.e. the normal modes of a physical system and the normal modes of a free ring polymer) reads as

$$H = K + \sum_{v=1}^{3N}\sum_{k=0}^{P-1}\frac{m_v(\omega_k^2 + \omega_{v,\text{full}}^2)}{2}\tilde{q}_v^{(k)2}, \tag{9}$$

$$\tilde{q}_v^{(k)} = \sum_{j=1}^{P} C_{jk}^P q_v^j \tag{10}$$

where k denotes NMs of a free ring polymer. Here and below, "full" index stands for the "expensive" potential energy surface which describes all interactions in a system, while "mol" stands for the "cheap" one. In case of spatially-localized contraction, a "cheap" potential describes only interactions within an adsorbate.

Contraction procedure. Given a ring polymer of P beads, one can contract it to a lower dimensionality. Many useful expressions can be found in [18]. Equations 21-22 from [18], rewritten in our notation:

$$q_v^{(j')} = \sum_{j=1}^{P'}(T_P^{P'})_{j'j}q_v^{(j)}, \tag{11}$$

where

$$(T_P^{P'})_{j'j} = \frac{1}{P}\sum_{k=-P'/2}^{P'/2} C_{j'k}^{P'}C_{jk}^P \tag{12}$$

is a contraction matrix from $(P \times 3N)$ to $(P' \times 3N)$-dimensional space. It performs transformation C^P to a Fourier space, there it truncates the high-order coefficients and transforms back to a lower-dimensional real space by $C^{P'}$. Similarly, we define an expansion matrix $T_{P'}^P$ from $(P' \times 3N)$ to $(P \times 3N)$-dimensional space. The expansion procedure is a reverse of a contraction with only difference: instead of truncating Fourier series, we have to expand it from P' to P terms. Since we don't have these coefficients, we set them to be zero. It can be shown that the potential energies

of the P- and P'-ring polymers are related as

$$\sum_{k=1}^{P} V(q_1^{(k)}, ..., q_{3N}^{(k)}) \approx \frac{P}{P'} \sum_{j=1}^{P'} V(q_1'^{(j)}, ..., q_{3N}'^{(j)}), \tag{13}$$

with respect to the accuracy of contraction.

The Hamiltonian after the SL-RPC is applied:

$$H = K + \sum_{\nu=1}^{3N} \left[\sum_{k=0}^{P'-1} \frac{m_\nu(\omega_k^2 + \omega_{\nu,\text{full}}^2)}{2} \tilde{q}_\nu^{(k)2} + \sum_{k=P'}^{P-1} \frac{m_\nu(\omega_k^2 + \omega_{\nu,\text{mol}}^2)}{2} \tilde{q}_\nu^{(k)2} \right]. \tag{14}$$

Then, the partition function of this system is

$$Q = \prod_{\nu=1}^{3N} \left[\prod_{k=0}^{P'-1} \frac{1}{\beta_P \hbar \sqrt{\omega_k^2 + \omega_{\nu,\text{full}}^2}} \prod_{k=P'}^{P-1} \frac{1}{\beta_P \hbar \sqrt{\omega_k^2 + \omega_{\nu,\text{mol}}^2}} \right] \tag{15}$$

The free energy of a (single) physical system:

$$\begin{aligned} F = -\frac{1}{\beta} \ln(Q) &== -\frac{1}{\beta} \sum_{\nu=1}^{3N} \left[-\sum_{k=0}^{P'-1} \ln(\beta_P \hbar \sqrt{\omega_k^2 + \omega_{\nu,\text{full}}^2}) - \sum_{k=P'}^{P-1} \ln(\beta_P \hbar \sqrt{\omega_k^2 + \omega_{\nu,\text{mol}}^2}) \right] = \\ &= \frac{3NP \ln(\beta_P \hbar)}{\beta} + \frac{1}{2\beta} \sum_{\nu=1}^{3N} \left[\sum_{k=0}^{P'-1} \ln(\omega_k^2 + \omega_{\nu,\text{full}}^2) + \sum_{k=P'}^{P-1} \ln(\omega_k^2 + \omega_{\nu,\text{mol}}^2) \right]. \end{aligned} \tag{16}$$

The free energy difference between SL-RPC and P beads calculated with full potential:

$$\delta F = (F^{RPC} - F^{P\ beads}) = \frac{1}{2\beta} \sum_{\nu=1}^{3N} \sum_{k=P'}^{P-1} \ln\left(\frac{\omega_k^2 + \omega_{\nu,\text{mol}}^2}{\omega_k^2 + \omega_{\nu,\text{full}}^2} \right) = \frac{1}{2\beta} \sum_{\nu=1}^{3N} \sum_{k=P'}^{P-1} \ln\left(1 + \frac{\omega_{\nu,\text{mol}}^2 - \omega_{\nu,\text{full}}^2}{\omega_k^2 + \omega_{\nu,\text{full}}^2} \right). \tag{17}$$

References

[1] V. G. Ruiz, W. Liu, E. Zojer, M. Scheffler, A. Tkatchenko, *Phys. Rev. Lett.* **2012**, *108*, 146103.

[2] T. Koitaya, S. Shimizu, K. Mukai, S. Yoshimoto, J. Yoshinobu, *The Journal of Chemical Physics* **2012**, *136*, 214705.

[3] P. Giannozzi, S. Baroni, N. Bonini, M. Calandra, R. Car, C. Cavazzoni, D. Ceresoli, G. L. Chiarotti, M. Cococcioni, I. Dabo, A. Dal Corso, S. de Gironcoli, S. Fabris, G. Fratesi, R. Gebauer, U. Gerstmann, C. Gougoussis, A. Kokalj, M. Lazzeri, L. Martin-Samos, N. Marzari, F. Mauri, R. Mazzarello, S. Paolini, A. Pasquarello, L. Paulatto, C. Sbraccia, S. Scandolo, G. Sclauzero, A. P. Seitsonen, A. Smogunov, P. Umari, R. M. Wentzcovitch, *Journal of Physics: Condensed Matter* **2009**, *21*, 395502.

[4] P. Giannozzi, O. Andreussi, T. Brumme, O. Bunau, M. B. Nardelli, M. Calandra, R. Car, C. Cavazzoni, D. Ceresoli, M. Cococcioni, N. Colonna, I. Carnimeo, A. Dal Corso, S. de Gironcoli, P. Delugas, R. A. DiStasio, A. Ferretti, A. Floris, G. Fratesi, G. Fugallo, R. Gebauer, U. Gerstmann, F. Giustino, T. Gorni, J. Jia, M. Kawamura, H.-Y. Ko, A. Kokalj, E. Küçükbenli, M. Lazzeri, M. Marsili, N. Marzari, F. Mauri, N. L. Nguyen, H.-V. Nguyen, A. Otero-de-la-

Roza, L. Paulatto, S. Poncé, D. Rocca, R. Sabatini, B. Santra, M. Schlipf, A. P. Seitsonen, A. Smogunov, I. Timrov, T. Thonhauser, P. Umari, N. Vast, X. Wu, S. Baroni, *Journal of Physics: Condensed Matter* **2017**, *29*, 465901.

[5] Y. Morikawa, H. Ishii, K. Seki, *Phys. Rev. B* **2004**, *69*, 041403.

[6] STATE code, `https://state-doc.readthedocs.io/en/latest/index.html`, Accessed: 2020-09-30.

[7] I. Hamada, *Phys. Rev. B* **2014**, *89*, 121103.

[8] M. Callsen, I. Hamada, *Phys. Rev. B* **2015**, *91*, 195103.

[9] G. Román-Pérez, J. M. Soler, *Phys. Rev. Lett.* **2009**, *103*, 096102.

[10] J. Wu, F. Gygi, *The Journal of Chemical Physics* **2012**, *136*, 224107.

[11] Y. Hamamoto, I. Hamada, K. Inagaki, Y. Morikawa, *Phys. Rev. B* **2016**, *93*, 245440.

[12] M. Otani, O. Sugino, *Phys. Rev. B* **2006**, *73*, 115407.

[13] I. Hamada, M. Otani, O. Sugino, Y. Morikawa, *Phys. Rev. B* **2009**, *80*, 165411.

[14] D. Vanderbilt, *Phys. Rev. B* **1990**, *41*, 7892–7895.

[15] E. B. Wilson, J. C. Decius, P. C. Cross, *Molecular vibrations: the theory of infrared and Raman vibrational spectra*, Dover Publications, **1980**.

[16] N. Ferri, R. A. DiStasio, A. Ambrosetti, R. Car, A. Tkatchenko, *Phys. Rev. Lett.* **2015**, *114*, 176802.

[17] Y. Litman, D. Donadio, M. Ceriotti, M. Rossi, *The Journal of Chemical Physics* **2018**, *148*, 102320.

[18] T. E. Markland, D. E. Manolopoulos, *The Journal of Chemical Physics* **2008**, *129*, 024105.